Article

A Highly Effective Protein Converting Strategy for Ultrasensitive Electrochemical Assay of Cystatin C

Zhe-Han Yang, Ying Zhuo, Ruo Yuan, and Yaqin Chai

Anal. Chem., **Just Accepted Manuscript** • DOI: 10.1021/acs.analchem.6b00210 • Publication Date (Web): 22 Apr 2016

A Highly Effective Protein Converting Strategy for Ultrasensitive Electrochemical Assay of Cystatin C

Zhe-Han Yang, Ying Zhuo, Ruo Yuan*, Ya-Qin Chai*

Key Laboratory of Luminescence and Real-Time Analytic Chemistry (Southwest University),Ministry of Education, College of Chemistry and Chemical Engineering, Southwest University, Chongqing 400715, China

ABSTRACT

In this work, a highly effective protein converting strategy based on immunoreaction-induced DNA strand displacement and T7 Exonuclease (T7 Exo)-assisted protein cyclic enzymatic amplification for ultrasensitive detection of cystatin C was described. Herein, $Au@Fe_3O_4$ as magnetic separator was labeled by antibody 1-conjungated DNA (DNA1) and the DNA substrate of T7 Exo (DNA3) which initially hybridized with output DNA (S1) to form a stable S1/DNA1 duplex (S1/DNA3). Antibody 2 was labeled by competing DNA (DNA 2). In the presence of cystatin C, sandwich immunoreaction would induce proximity hybridization between DNA2 and DNA3 and thus displace S1 from S1/DNA3 duplex with formation of a stable DNA2/DNA3 duplex, realizing the conversion of input target cystatin C into output S1. To enhance the conversion ratio, the DNA2/DNA3 duplex was then digested by T7 Exo with release of DNA2 which could act as competing DNA again to displace S1 from the S1/DNA3 duplex in adjacent locations and initiate another cleavage reaction. Through such a cyclic process, each input cystatin C could induce more than one output S1, enhancing detection sensitivity. A hairpin DNA modified electrode was used to capture the output S1, and then a hybridization chain reaction is triggered on biosensor surface. Then, thionine as electron mediator was embed into the dsDNA polymers to produce detection signal. The electrochemical biosensor exhibited a much wider linear range of 0.01 pg mL^{-1} to 30 ng mL^{-1} with low detection limit of 3 fg mL^{-1}. Moreover, this method introduced protein unrelated to nucleic

acids into the realm of potential inputs for translation, which might create a new immunoassay method for sensitive detection of protein.

INTRODUCTION

The detection of proteins plays the key roles in early clinical diagnosis and disease prevention.[1,2] Typically, protein recognition elements include aptamer,[3-5] peptide[6] and antibody.[7,8] So far, only a few aptamers or peptides have shown potential for protein detection especially with the traditional "sandwich" structure. Probably the most important scientific reason is related to difficulties in the selection of highly-selective aptamers or peptides for different protein targets and measurement conditions.[9] As a result, antibodies are still main recognition elements in the protein detection. In the past decades, various immunoassay methods based on nanomaterials- and enzyme-related amplification strategy have been reported.[10-14] Recently, DNA-based amplification strategies are introduced to immunoassay by using single-stranded DNA (ssDNA) labeled antibody as probe, in which ssDNA could further induce DNA assembly on each immunocomplex.[15-17] These methods enable employment of many ripe DNA nanotechnology strategies such as rolling circle amplification, hybridization chain reaction (HCR), and nicking enzyme recycling amplification for protein detection.[18-21] Inspired by these, it will be valuable if a highly effective protein converting system that allow conversion of input target protein into output ssDNA, which can induce further DNA assembly more easily and simply compared with the DNA modified with protein in the view of the steric effect.

Molecular conversion is often applied in nucleic acids as a result of their predictable sequence-specific hybridization properties, ease of preparation in vitro using chemical synthesis, and numerous functions in biology.[22] A classic example of molecular conversion based on nucleic acids is PCR-independent isothermal strategy which has widen implement in DNA detection and gene diagnostics.[23,24] In addition, there are still great efforts that directed toward molecular conversion on the basis of nucleic acids. For example, Picuri and coworker designed universal molecular conversions that efficiently translate several different biologically relevant input sequences into a unique output in 5 min.[22] Molecular conversion also showed great potential of sensitive assay of DNA or RNA, in which input target DNA or RNA converted into a unique output ssDNA to obtain detection signal.[26-28] Moreover, small molecules were used to trigger changes in DNA structures by incorporating structure-switching aptamers.[29,30] However, to date, molecular conversion based on protein recognition, especially immune recognition is rarely reported. Recently, proximity ligation assay (PLA) that binding of two affinity ligands (aptamers and nucleic acids modified antibodies) to the same target molecule resulted in binding-induced DNA assemblies have been reported.[31-37] A unique advantage of this approach is the incorporation of DNA technology to immunoreaction, which can extend the generality of protein detection by immunoreaction. Among various PLA-based strategies, protein recognition-induced DNA strand displacement may be a noble strategy because it allow conversion of the input target protein into a unique

output ssDNA.[38,39] However, the conversion ratio of the reported PLA-based translation strategy is 1:1, limiting the sensitivity of PLA-based conversion in protein detection. Thus, we aimed to construct a conversion strategy with high conversion ratio for sensitive detection protein.

Cystatin C, a nonglycosylated cysteine protease inhibitor, is produced at a constant rate by nucleated cells and freely filtered by the renal glomerulus.[40,41] Cystatin C has been acknowledged as a marker of assessed risk of death from myocardial infarction, stroke, and metabolic syndrome.[42-44] In this work, we presented a highly effective protein converting strategy for ultrasensitive detection of cystatin C based on immunoreaction-induced DNA strand displacement and T7 Exonuclease (T7 Exo)-assisted protein cyclic enzymatic amplification. Firstly, DNA 1 and DNA 2 were linked to antibody 1 (DNA1-Ab1) and antibody 2 (DNA2-Ab2) respectively by EDC and NHS for preparation of two affinity probes. In order to realize protein conversion, DNA1-Ab1 and DNA 3-hybridized with DNA S1 (S1/DNA3) were initially immobilized on the surface of $Au@Fe_3O_4$ by Au-S bond for further magnetic separation. In the presence of cystatin C and DNA2-Ab2, sandwich immunoreaction would bring DNA2 into close proximity of S1/DNA3 duplex, and then DNA2 served as competing DNA to displace S1 from S1/DNA3 duplex with formation of DNA2/DNA3 duplex. To enhance the conversion ratio, the DNA2/DNA3 duplex was digested by T7 Exo which only cleaves the 5' recessed DNA strand from the duplex with release of DNA2. The DNA2 could act as competing DNA again to displace S1

from the S1/DNA3 duplex in adjacent locations and initiate another reaction cycle. As a result, a protein molecular could induce more than one output S1, enhancing the detection sensitivity significantly. The output S1 was obtained through a magnetic separation process, and then dropped on the modified electrode to trigger further DNA assembly. Au nanoparticles (AuNPs) and nano-C_{60} decorated glassy carbon electrode (GCE) with high specific surface area and the active interface was used as platform for thiol-modified capture hairpin DNA (H1) immobilization. The stem-loop structure of capture probe H1 was open with the help of S1, and then the newly emerging sequence of H1 could open hairpin H2. The exposed part of H2 could serve as an initiator to trigger HCR in the presence of H3 and H4, which brought the formation of extended double-stranded DNA (dsDNA) polymers. Afterwards, a large amount of thionine (Thi) as electron mediator could be embed into the dsDNA polymers through electrostatic interaction, achieving detection signal. Therefore, the sensitivity of the proposed method for detection of cystatin C could be significantly enhanced by using immunoreaction-induced DNA strand displacement, T7 Exo-assisted cystatin C cyclic and HCR as signal amplification protocol.

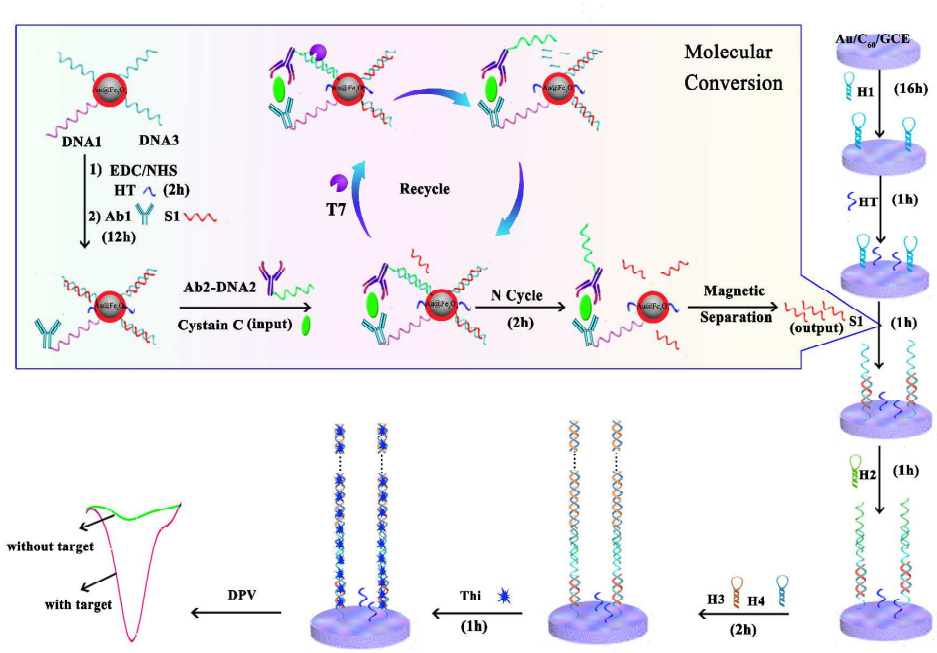

Scheme 1. Electrochemical detection of cystatin C by combining a protein converting strategy with T7 Exo-assisted protein cyclic enzymatic amplification.

EXPERIMENTAL SECTION

Chemicals and biochemical. Ab1, Ab2 and antigen cystatin C were purchased from Elabscience Bio. Co. Ltd. (Wuhan, China). T7 Exo was achieved from New England Biolabs Ltd. (Beijing, China). Fe_3O_4 magnetic beads was purchased from BaseLine Chrom Tech Research Centre (Tanjing, China). Fullerene (C_{60}) were obtained from Nanjing XFNANO Materials Tech Co., Ltd. (Nanjing, China). N-(3-dimethylaminopropyl)-N-ethylcarbodiimeidehydride (EDC) and N-hydroxysuccinimide (NHS) were obtained from Shanghai Medpep Co. Ltd (Shanghai, China). Hexanethiol (HT), Thi and gold chloride ($HAuCl_4 \cdot 4H_2O$) were

supplied by Sigma (St. Louis, MO, USA). 0.1 M PBS (pH 7.0) containing 0.1 M Na_2HPO_4, 0.1 M NaH_2PO_4 and 2 mM $MgCl_2$ was used as working buffer solution. Hybridization buffer (pH 7.0) containing 10 mM tris-HCl, 1.0 mM EDTA, 1.0 M NaCl was used as binding solution.

All synthetic oligonucleotides were ordered from Shanghai Sangon Biological Engineering Technology and Services Co., Ltd. (Shanghai, China), and the sequences were listed as follow:

name	sequences*(5′→3′)
H1	GCCTAGCGGCGCAGCATTCTAAGGCGACATCCGCTAGGCTTAAAG-$(CH_2)_6$-SH
H2	AAT GCT GCG CCG GTA GGC ATT TTA GCC TAC CGG CGC
H3	GCG CCG GTA GGC TAA CAA AGT TTA GCC TAC
H4	TTA GCC TAC CGG CGC GTA GGC TAA ACT TTG
S1	CTTTAAGCCTAGCGGATGTT
DNA1	SH-TTTTTTTTTTTTTTTTTTTTTTTTTTTTTTTTTTTTTTTTTTTTTTTTTTTTTT TTTTTTTTTTTTTTTTTTTTTTTTTT-COOH
DNA2	GCCATGCGGATGTTTGTGTTTTTTTTTTTTTTTTTTTTTTTTTTTTTTTTTT TTTTTTTTTTTTTTTTTTTTTTTTTT-NH_2
DNA3	CACAAACATCCGCATGGCTTAAAGTTT-$(CH_2)_6$-SH

Apparatus and measurements. A conversional three-electrode system including a platinum wire auxiliary electrode, glassy carbon electrode (GCE, Φ = 4 mm) as working electrode and a saturated calomel reference electrode was applied to performed all experiments. Electrochemical measurements were carried out on CHI 660D electrochemical workstation (Shanghai Chenhua instrument Co., Ltd, China).

Gel electrophoresis was conducted using a DYY-8C electrophoretic apparatus (Beijing, Wo De Life Sciences Instrument Co., Ltd, China). Morphologies of the samples were characterized by using transmission electron 124 microscopy (TEM; H600, Hitachi, Japan) and scanning electron microscopy (SEM, S-4800, Hitachi, Japan).

Preparation of DNA2-Ab2. The DNA2 labeled Ab2 (DNA2-Ab2) was prepared by the following steps. Firstly, 5.0 μL of 4.75 mg mL^{-1} Ab2 antibody was initially incubated with 90 μL of PBS (pH 7.4) containing 20 mM EDC and 5 mM NHS for 2 h at 4 °C. Secondly, the amino-modified single-stranded DNA2 (10 μL, 100 μM) was added into the above-mentioned PBS (pH 7.4) and reacted for 12 h at 4 °C. Following that, the unconjugated DNA2 and Ab2 were removed by ultrafiltration with 20,000 MW cutoff membrane. Finally, the Ab2-conjugated DNA2 conjugates were dissolved in 100 μL of PBS buffer (pH 7.0) for further use (SDS-polyacrylamide gel electrophoresis (SDS-PAGE) was conducted to investigate the coupling efficiency and the product purity shown in Fig. S1, Supporting Information).

Fabrication of cystatin C assay. Scheme 1 showed the procedure of the biosensor for electrochemical assay of cystatin C. First, 100 μL of Tris-HCl buffer containing 1% (*w*/*w*) Au@Fe_3O_4, 2 μM thiol-modified single-stranded DNA1, 2 μM thiolated single-stranded DNA3 was reacted at room temperature for 16 h. The supernatant was removed by magnetic force, followed by adding 20 mM EDC and 5 mM NHS to activate the carboxyl group of DNA1, and 1mM HT to block nonspecific binding sites.

After a magnetic separation, S1 (50 μL, 4 μM) and Ab1 (50 μL, 4 μM) were added and incubated for 12 h, thus the S1/DNA3 duplex and DNA1-Ab1 could be formed on the surface of $Au@Fe_3O_4$. Then, non-hybridized S1 and non-reaction Ab1 were removed. The biocomplex incubated with 20 μL of DNA2-Ab2, 40 μL 30 U mL^{-1} T7 Exo and 40 μL of cystatin C solution with various concentrations at 37 °C for 120 min. Finally, solutions containing various concentrations of S1 could be collected by a magnetic field and used for triggering DNA assembly on the surface of electrode.

Before using, a pretreat process for all the hairpin oligonucleotides was conducted via warming the solution to 95 °C for 2 min and then cooling to room temperature. To obtain a mirror-like surface, GCE was polished with 0.3 and 0.05 μm alumina powder respectively and sonicated with double distilled water. Then, 6 μL nano-C_{60} (Fig. S2 A, Supporting Information) suspension prepared by an ultrasound assisted solution-phase conversion process according to the literature[45] was cast onto the treated electrode surface and dried in air to form a homogeneous film. Next, the nano-C_{60} modified electrode (C_{60}/GCE) was immersed into the solution of $HAuCl_4$ (5 mM) and K_2SO_4 (5 mM) and an electrodeposition was carried out at a constant potential of -0.35 V for 40 s to obtain AuNPs layer (Fig. S2 B, Supporting Information). Following that, 10 μL of thiol-modified H1 (2 μM) was dropped onto the Au/C_{60} layer for 16 h at room temperature, leading to assembling H1 on the modified electrode. Subsequently, the electrode surface was rinsed with double distilled water and blocked with 1.0 mM HT for 1 h. After that, 10 μL of mixture

containing different concentrations of the preceding released S1 and 10 μL of H2 (2 μM) were dropped onto the modified electrode and incubated for 60 min at room temperature. After rinsing with double distilled water, the electrode was incubated with 10 μL of H3 (2 μM) and 10 μL of H4 (2 μM) at room temperature for 120 min. Ultimately, Thi (10 μL, 1.0 mM) as an electron mediator was embed into the dsDNA polymers via electrostatic adsorption.

Non-denaturing polyacrylamide gel electrophoresis (PAGE). The notches of the freshly prepared non-denaturing polyacrylamide gel (16%) was used to load the samples, and electrophoresis was conducted at 120 V for 90 min in 1 × TBE buffer. Before loading, DNA samples were mixed with DNA loading buffer on a volume ratio of 5:1. After separation, the electrophoresis image was obtained under UV light.

RESULTS AND DISSCUSSION

Mechanism of the target cystatin C conversion. The principle of electrochemical biosensor based on a target cystatin C converting system is illustrated in Scheme 1. The process of target cystatin C conversion is composed of cystatin C-recognition, immunoreaction-driven DNA strand displacement, and T7 Exo-assisted cyclic enzymatic amplification. Cystatin C-recognition is obtained by two ssDNA-labeled antibodies recognize to the cystatin C. Thiolated DNA 1-labeled Ab1 (DNA1-Ab1) is immobilized onto the surface of Au@Fe_3O_4, which serve as the scaffold and separator for the protein conversion. DNA2 as competing DNA in protein conversion event is

linked to Ab2. S1 is initially hybridized to DNA3 which is also immobilized on the surface of Au@Fe_3O_4 with formation S1/DNA3 duplex. As shown in scheme 2, the complementary sequences between DNA2 and DNA3 are two nucleotides shorter than between S1 and DNA3. Therefore, displacement of S1 by DNA2 is minimal in the absence of cystatin C. However, when cystatin C existed, the binding of the cystatin C to the two antibodies brings DNA2 into close proximity to the S1/DNA3 duplex and then accelerate the strand-displacement reaction between DNA2 and S1. Through such process, S1 can be released from the scaffold to solution. Moreover, T7 Exo-assisted target cyclic enzymatic amplification is designed for enhancement the amount of output S1. Briefly, since T7 Exo only cleaves the 5' recess DNA strand from the duplex, DNA2 can be released from DNA2/DNA3 duplex in the presence of T7 Exo, and then act as competing DNA to displace S1 from the other S1/DNA3 duplex in adjacent locations. As a consequence, T7 Exo initiate a new cleavage reaction. The subsequent detection signal can be generated by using S1 to trigger further DNA assembly on the surface of electrode.

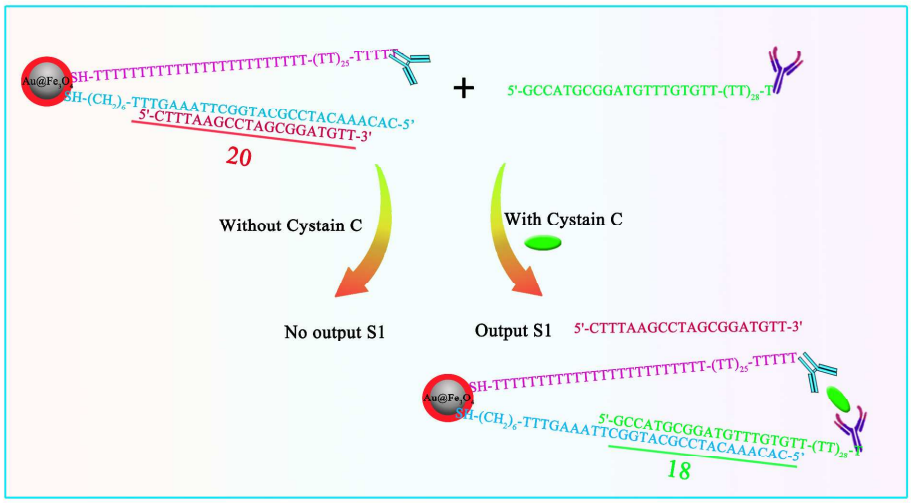

Scheme 2. General principle of protein converting strategy.

Characterization of biosensor. To characterize the biosensor preparation procedure, electrochemical impedance spectroscopy (EIS) measurements were conducted. As shown in Fig. 1A, the C_{60} modified GCE showed a much larger R_{et} (curve b) than bare GCE (curve a). After AuNPs were electrodeposited on C_{60}/GCE, a decrease in the R_{et} value was obtained (curve c). When Au/C_{60}/GCE was modified by H1, an increase in the R_{et} value was achieved owing to the negatively charged of H1 (curve d). A further increase of R_{et} could be observed when the surface was blocked with HT (curve e), suggesting that the biosensor was successfully prepared. When S1 and H2 were dropped, the hybridization events among S1, H1 and H2 led to the increase of R_{et} (curve f). The complementary sequence of H2 then assembled with the mixture of H3 and H4 and the R_{et} was further increased (curve g), which was ascribed to the introduction of more negative charges on the electron surface upon the formation of the dsDNA polymers (to further provide information about the

preparation of the biosensor, the CVs was used to provide detailed information shown in Fig. S3, Supporting Information).

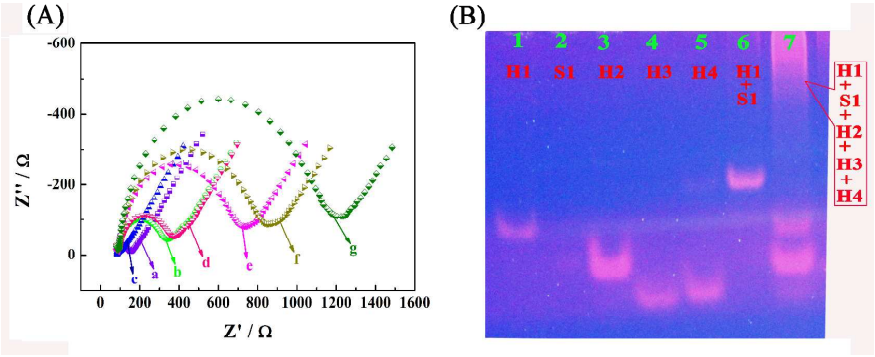

Figure 1. (A) EIS of various modified electrode in 5.0 mM $[Fe(CN)_6]^{3-/4-}$: (a) bare GCE, (b) C_{60}/GCE, (c) AuNP/C_{60}/GCE, (d) H1/AuNP/C_{60}/GCE, (e) HT/H1/AuNP/C_{60}/GCE, (f) S1/HT//H1/AuNP/C_{60}/GCE, (g) H3, H4/H2/S1/H1/AuNP/C_{60}/GCE. (B) PAGE analysis of different samples, Line 1: H1; Line2: S1; Line 3: H2; Line 4: H3; Line 5: H4; Line 6: a mixture of H1 and S1; Line 7: a mixture of H1, S1, H2, H3, and H4.

PAGE analysis. PAGE (16%) was applied to verify S1 trigger-DNA assembly. The H1, S1, H2, H3 and H4 in lanes 1, 2, 3, 4 and 5 respectively, exhibited a different single band (Fig. 1B). Lane 6 showed the PAGE result for sequential hybridization of H1 with S1 at the same concentration of 2 μM. As expected, a band with slower mobility could be observed (lane 6 *vs*. 1, 2), suggesting successful hybridizations between H1 and S1. When added H2, H3 and H4 into the dsDNA between H1 and S1, the exposed sequence of H1 could open hairpin H2 and then trigger HCR event, yielding long dsDNA molecule. As a consequence, a band with very slow mobility

(lane 7) could be observed, which indicated the successful formation long dsDNA molecule.

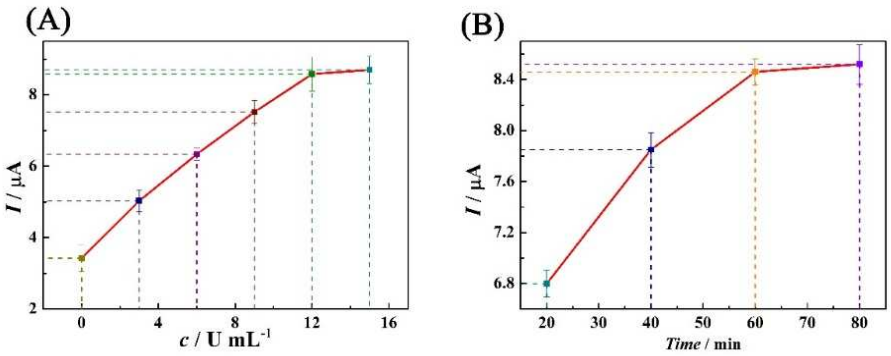

Figure 2. (A) influence of the concentration of T7 Exo on the biosensor, (B) effect of the time of cleavage of T7 Exo on the biosensor.

Optimization of detection conditions. Because T7 Exo-assisted target cyclic enzymatic amplification is required to ensure the efficiency of cleavage of T7 Exo, the effect of the concentration of T7 Exo and the enzymatic cleavage time were optimized in this study. The proposed biosensor was assessed by using DPV with six T7 Exo concentrations (3.0, 6.0, 9.0, 12.0, 15.0 U mL^{-1}) at 5 ng mL^{-1} cystatin C. With increment of the concentration of T7 Exo, the current response increased. Then, a plateaus was observed after the concentration of T7 Exo more than 12.0 U mL^{-1}. Thus, the optimal concentration of T7 Exo was 12 U mL^{-1}, which was adopted in the subsequent work (Fig. 2A). Under above optimal condition, the influence of the enzymatic cleavage time was also investigated intermittently (every 20 min). It was obvious that the current intensity increased with prolonged cleavage time and then

tended to level off after 60 mins, demonstrating that 60 min was enough for enzymatic cleavage (Fig. 2B).

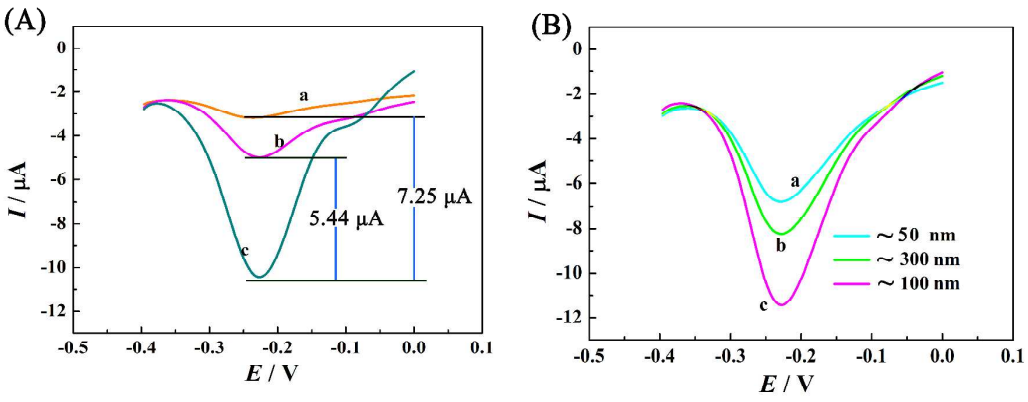

Figure 3. (A) The DPV response of the biosensor incubated with 0 ng mL^{-1} (curve a), 5 ng mL^{-1} without (curve b) and with (curve c) use of T7 Exo-assisted cystatin C cyclic enzymatic amplification strategy. (B) The DPV response after the sandwich format immunoreaction of the proposed biosensor with different size of Au@Fe_3O_4 (curve a: ~50 nm, Curve b: ~300 nm, curve c: ~100 nm).

Comparison of current response under different conditions. The concentration of target cystatin C was investigated by conversion of cystatin C into S1 output which was used to induce DNA assembly on the surface of electrode, resulting in electrochemical signal output. And T7 Exo-assisted target cyclic was designed for enhancing the conversion efficiency for electrochemical signal amplification. To clarify these two points, the prepared biosensor was used for detection of 0 and 5 ng mL^{-1} cystatin C respectively. As seen from Fig. 3A, curve a present the DPV peak current (3.19 μA) of the proposed biosensor incubated with 0 ng mL^{-1} cystatin C.

When the biosensor was incubated with 5 ng mL^{-1} cystatin C, the peak current increased to 10.44 μA (curve c), suggesting that target cystatin C could successfully convert into S1 output. However, when the biosensor was incubated with 5 ng mL^{-1} cystatin C without use of T7 Exo-assisted target cyclic, only 5.00 μA peak current was obtained (curve b). The reason might be ascribed to the fact that T7 Exo-assisted target cyclic could improve the conversion efficiency, resulting in electrochemical signal amplification.

Estimation of effect of the size of the Au@Fe_3O_4 for detection signal. Since the process of immunoreaction-driven DNA strand displacement and T7 Exo-assisted target cyclic occurred on the surface of Au@Fe_3O_4, steric effect might affect the detection signal. To investigate this issue, different size of the Au@Fe_3O_4 (~50 nm, ~100 nm, and ~300 nm, Fig. S3, Supporting Information) was used as platform for immobilizing biomolecular and the performance of biosensor was evaluated by DPV experiment. As seen from Fig. 3B, compared with Au@Fe_3O_4 with diameter of about 50 nm, the biosensor used Au@Fe_3O_4 with diameter of about 100 nm as platform showed much higher current response. The result indicated that platform with diameter of about 100 nm showed littler steric effect on DNA strand displacement as well as T7 Exo-assisted target cyclic, which was beneficial to protein conversion in this system. However, when much larger size of Au@Fe_3O_4 (~300 nm) was used as platform, lower current response was observed in comparison with that of Au@Fe_3O_4 with about 100 nm, suggesting that platform with use of Au@Fe_3O_4 with about 300

nm showed greater steric hindrance than that of $Au@Fe_3O_4$ with about 100 nm. Therefore, we used $Au@Fe_3O_4$ with about 100 nm as platform for immobilizing biomolecular in this work.

The performance of the biosensor. Under optimal conditions, the proposed biosensor was incubated with various concentrations of cystatin C standard solution and performed by DPV. As shown in Fig. 4. The peak current of Thi increased with increment cystatin C concentration with a linear range from 0.01 pg mL^{-1} to 30 pg mL^{-1} and the linear regression equation was $I = 0.3096\ c + 4.412$ ($R^2 = 0.9809$) with a detection limit of 3.1 fg mL^{-1} (Fig. 4A). For comparison, the performance of biosensor without using T7 Exo-assisted target cyclic enzymatic amplification strategy was also investigated. A linear range of 1.0 pg mL^{-1} to 30 pg mL^{-1} with a detection limitation of 0.3 pg mL^{-1} was obtained ($I = 0.1700\ c + 0.5171$, $R^2 = 0.9801$) (Fig. 4B). The higher sensitivity and wider linear range demonstrated that the T7 Exo-assisted target cyclic enzymatic amplification strategy could improve the sensitivity of the biosensor for cystatin C detection. The performance was also compared with some reported methods based on PLA for protein detection. The results indicated that the detection sensitivity was acceptable and competitive (Table S1, Supporting Information).

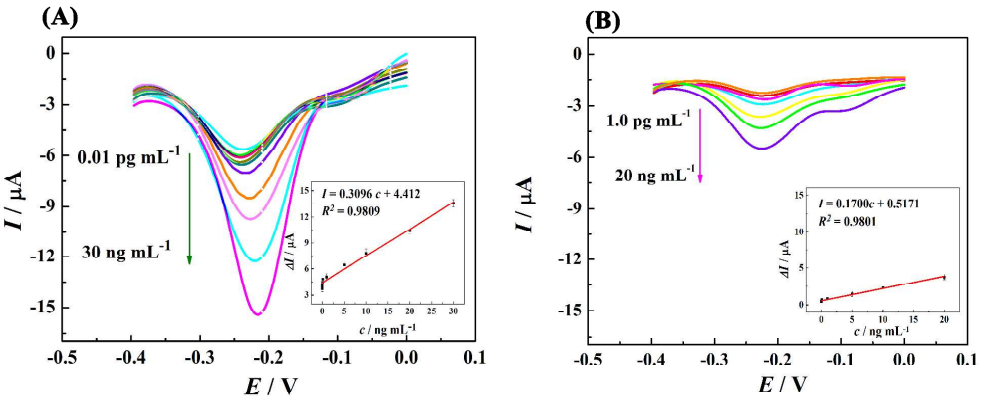

Figure 4. DPV response of the biosensor with (A) and without (B) use of T7 Exo-assisted target cyclic enzymatic amplification strategy when incubation with a series of concentrations of cystatin C. (insert: the biosensor calibration curves with and without use of T7 Exo-assisted target cyclic enzymatic amplification strategy for 0.01 pg mL^{-1} to 30 ng mL^{-1} and 1.0 pg mL^{-1} to 20 ng mL^{-1} respectively).

To evaluate the specificity of the biosensor, four possible interferences including influenza, thrombin (TB), hemoglobin (Hb) and matrix metalloproteinase-2 (MMP-2) were assessed under the same experimental conditions. Compared with the blank test, there were almost no difference of DPV response in the detection of influenza (100 nM), TB (100 nM), Hb (100 nM) and MMP-2 (100 nM) shown in Fig. 5A. However, when biosensor incubated with 5 ng mL^{-1} cystatin C, high DPV response was achieved. Meanwhile, while 5 ng mL^{-1} cystatin C coexisted with interferences (100 nM) in the buffer, no obvious signal change existed in comparison with the case of only cystatin C. The result indicated the high specificity of this biosensor for cystatin C assay.

To assess the inter-assay precision, five of the biosensor with 5 ng mL^{-1} cystatin C were investigated under the same detection condition. Similar electrochemical response was obtained and the relative standard deviation (RSD) was 6.4%. Besides, the intra-assay precision was also assessed via detecting the same biosensor for five times and the RSD was 7.2%. These two results demonstrated that the reproducibility was acceptable.

To evaluate the stability of the proposed biosensor, successive cyclic scan was conducted. As shown in Fig. 5B, compared with initial electrochemical response, the current intensity decreased only about 10.7% after 80 cycles' continuous CV measurement. In addition, the long-term stability experiment was also performed via storing the biosensor at 4 ºC and assaying every four days by DPV. Five of biosensors with 5 ng mL^{-1} cystatin C were evaluated under the same assay conditions. After 20 days, the DPV response retained 94.5%, 91.2%, 90.7%, 89.1% and 93.7% of their initial current, indicating that the biosensor had good stability. The results demonstrated that dsDNA polymers intercalated with Thi could maintain favorable electrochemical activity for cystatin C analysis.

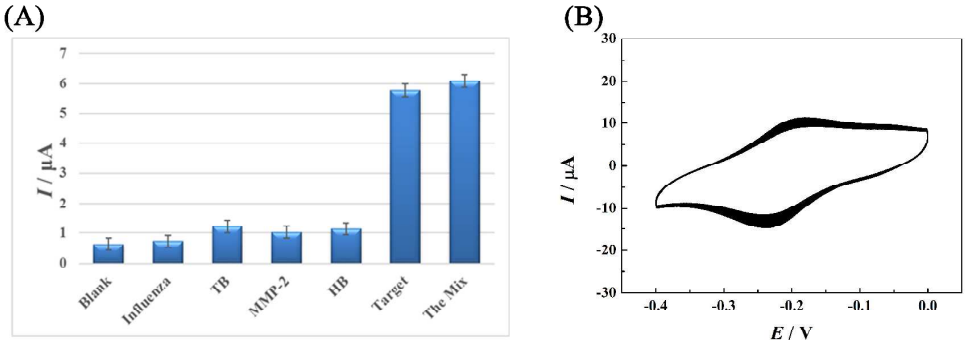

Figure 5. (A) The specificity of the electrochemical biosensor. (B) Stability of the proposed biosensor.

Clinical serum samples analysis. The recovery experiment was performed to assess the analytical reliability and application potential of the newly developed biosensor for cystatin C assay. Briefly, the healthy human serum sample was used to prepare various concentrations of cystatin C. Then, biosensor incubated with the above samples was investigated to assess the influence of the serum samples for cystatin C detection. Table 1 showed the experimental result, it could be see that the recovery was varying from 93% to 110% and RSDs was ranging from 2.9% to 9.3%. These results suggested that detection of cystatin C in serum samples was promising.

Table 1 Recovery results of the proposed biosensor in human serum

Sample no.	Added/ (ng mL^{-1})	Found/ (ng mL^{-1})	Recovery/%	RSD/%
1	0.001	0.0011	110	6.2
2	0.1	0.095	95	2.9
3	5.0	4.6	98	6.2
4	10.0	9.3	93	9.3
5	20.0	18.9	94.5	7.2

CONCUSION

In summary, we developed a protein translating strategy for electrochemical detection of cystatin C based on immunoreaction-induced DNA strand displacement, in which the simultaneous recognition of the target by two nucleic acid-labeled

antibodies was used to induce DNA strand displacement. Through this conversion construct and magnetic separation, cystatin C detection could be converted to the DNA assay which extend method for protein detection from traditional immunoassay. Additionally, this method introduced target protein unrelated to nucleic acids into the realm of potential inputs for translation via using nucleic acid-labeled antibodies as recognition elements. Because of antibody specific recognition of target protein, it was possible to extend this strategy to detection various proteins, allowing the detection of a broad spectrum of proteins. In view of these advantages, immunoreaction-induced DNA strand displacement might create a new immunoassay method for sensitive detection of proteins.

ASSOCIATED CONTENT

Supporting Information

Additional information as noted in text.

AUTHOR INFORMATION

*Tel.: +86-23-68252277; Fax: +86-23-68253172. E-mail address: yuanruo@swu.edu.cn (R. Yuan), yqchai@swu.edu.cn (Y. Q. Chai)

Notes

The authors declare no competing financial interest.

ACKNOWLEDGMENTS

The authors are grateful for the National Natural Science Foundation of China (21575116, 21275119, 51473136), the Fundamental Research Funds for the Central Universities (XDJK2015A002, XDJK2014A012), China.

REFERENCES

(1) Tran, T. N. N.; Cui, J.; Hartman, M. R.; Peng, S.; Funabashi, H.; Duan, F.; Yang, D.; March, J. C.; Lis, J. T.; Cui, H.; Luo D. *J. Am. Chem. Soc.* **2013**, *135*, 14008-14011.

(2) Chikkaveeraiah, B. V.; Bhirde, A. A.; Morgan, N. Y.; Eden, H. S.; Chen X. *ACS Nano* **2012**, 6, 6546-6561.

(3) Han, D.; Zhu, Z.; Wu, C.; Peng, L.; Zhou, L.; Gulbakan, B.; Zhu, G.; Williams, K. R.; Tan W. *J. Am. Chem. Soc.* **2012**, *134*, 20797-20804.

(4) Chen, F.; Gülbakana, B.; Zenobi, R. *Chem. Sci.* **2013**, *4*, 4071-4078.

(5) Yang, Z.; Zhuo, Y.; Yuan, R.; Chai, Y. *ACS Appl. Mater. Interfaces* **2015**, *7*, 10308-10315.

(6) London, N.; Raveh, B.; Cohen, E.; Fathi G.; Schueler-Furman, O. *Nucleic Acids Res.* **2011**, *39*, 249-253.

(7) Penga, H.P.; Lee, K. H.; Jian, J. W.; Yang A. S. Proc. Natl. Acad. Sci. USA **2014**, *7*, 2656-2665.

(8) Wu, S.; Liu, H.; Liang, X. M.; Wu, X.; Wang, B.; Zhang, Q. *Anal. Chem.* **2014**, *86*, 4271-4277.

(9) Chen, A.; Chatterjee S.; *Chem. Soc. Rev.* **2013**, *42*, 5425-5438.

(10) Zhao, Y.; Liu, L.; Kong, D.; Kuang, H.; Wang, L.; Xu, C. *ACS Appl. Mater. Interfaces* **2014**, *6*, 21178-21183.

(11) Chen, L.; Zeng, X.; Si, P.; Chen, Y.; Chi, Y.; Kim, D. H.; Chen, G. *Anal. Chem.* **2014**, *86*, 4188-4195.

(12) Luo, Y.; Liu, T.; Zhu, J.; Kong, L.; Wang, W.; Tan L. *Anal. Chem.* **2015**, *87*, 11277-11284.

(13) Johari-Ahar, M.; Rashidi, M. R.; Barar, J.; Aghaie, M.; Mohammadnejad, D.; Ramazani, A.; Karami, P.; Coukosde, G.; Omid, Y. *Nanoscale* **2015**, *7*, 3768-3779.

(14) Su, S.; Zou, M.; Zhao, H.; Yuan, C.; Xu, Y.; Zhang, C.; Wang, L.; Fan C.; Wang, L. *Nanoscale* **2015**, *7*, 19129-19135.

(15) Hu, J.; Wang, T.; Kim, J.; Shannon, C.; Easley, C. J. *J. Am. Chem. Soc.* **2012**, *134*, 7066-7072.

(16) Liu B.; Chen J.; Wei Q.; Zhang, B.; Zhang, L.; Tang, D. *Biosens. Bioelectron.* **2015**, *69*, 241-248.

(17) Zong, C.; Wu, J.; Liu, M.; Yang, L.; Liu, L.; Yan, F.; Ju, H. *Anal. Chem.* **2014**, *86*, 5573-5578.

(18) Leuchowius, K. *Nat. Methods* **2006**, *3*, 995-1000.

(19) Bi, S.; Zhao, T. T.; Luo, B. Y.; Zhu, J. J. *Chem. Commun.* **2013**, *49*, 6906-6908.

(20) Tang, L. H.; Liu, Y.; Ali, M. M.; Kang, D. K.; Zhao, W. A.; Li, J.H. *Anal. Chem*. **2012**, *84*, 4711-4717.

(21) Wang, L. J.; Zhang, Y.; Zhang, C. Y. *Anal. Chem*. **2013**, *85*, 11509-11517.

(22) Picuri, J. M.; Frezza, B. M.; Reza Ghadiri M. *J. Am. Chem. Soc*. **2009**, *131*, 9368-9377.

(23) Rosi, N. L.; Mirkin, C. A. *Chem. Rev*. **2005**, *105*, 1547-1562.

(24) Rothemund, P. W. *Nature* **2006**, *440*, 297-302.

(25) Beyer, S.; Simmel, F. C. *Nucleic Acids Res.* **2006**, *34*, 1581-1587.

(26) Xing, Y.; Yang, Z.; Liu, D. *Angew. Chem. Int. Ed.* **2011**, *123*, 12140-12142;

(27) Wu, X.; Chai, Y.; Zhang, P.; Yuan, R. *ACS Appl. Mater. Interfaces* **2015**, *7*, 713-720.

(28) Chen, Y.; Xiang, Y.; Yuan R.; Chai, Y. *Nanoscale* **2015**, *7*, 981-986.

(29) Xing, Y.; Yang, Z.; Liu, D. *Angew. Chem. Int. Ed.* **2011**, *50*, 11934-11936.

(30) Bai L.; Chai Y.; Pu, X.; Yuan, R. *Nanoscale* **2014**, *6*, 2902-2908.

(31) Hu, J.; Yu, Y.; Brooks, J. C.; Godwin, L.A.; Somasundaram, S.; Torabinejad, F.; Kim, J.; Shannon, C.; Easley, C. J. *J. Am. Chem. Soc.* **2014**, *136*, 8467-8474

(32) Zhang, Y. L.; Huang, Y.; Jiang, J. H. Shen, G. L.; Yu R. Q.; *J. Am. Chem. Soc.* **2007**, *129*, 15448-15449.

(33) Ren, K.; Wu, J.; Ju, H.; Yan, F. *Anal. Chem.* **2015**, *87*, 1694-1700.

(34) Zhang, H.; Li, F.; Dever, B.; Li, X. F.; Le, X. C. *Chem. Rev.* **2013**, *113*, 2812-2841.

(35) Tang, Y.; Lin, Y.; Yang, X.; Wang, Z.; Le, X. C.; Li, F. *Anal. Chem.* **2015**, *87*, 8063-8066.

(36) Li, F.; Lin, Y.; Le, X. C. *Anal. Chem.* **2013**, *85*, 10835-10841.

(37) Li, F.; Zhang, H.; Wang, Z.; Li, X.; Li, X. F.; Le, X. C. *J. Am. Chem. Soc.* **2013**, *135*, 2443-2446.

(38) Li, F.; Zhang, H.; Lai, C.; Li, X. F.; Le, X. C. *Angew. Chem. Int. Ed.* **2012**, *51*, 9317-9320.

(39) Zhang, L.; Zhang, K.; Liu, G.; Liu, M.; Liu, Y.; Li, J. *Anal. Chem*. **2015**, *87*, 5677-5682.

(40) Odutayo, A.; Cherney, D. *Clin. Nephrol.* **2012**, *78*, 64-75.

(41) Meyer, K.; Ueland, P. M. *Anal. Chem.* **2014**, *86*, 5807-5814.

(42) Hojs Fabjan, T.; Penko, M.; Hojs, R. *Renal Failure* **2014**, *36*, 81-86.

(43) Nedelkov, D.; Shaik, S.; Trenchevska, O.; Aleksovski, V.; Mitrevski, A.; Stojanoski, K. *Open Proteomics J.* **2008**, *1*, 54-58.

(44) Levy, E.; Jaskolski, M.; Grubb, A. *Brain Pathol.* **2006**, *16*, 60-70.

(45) Andrievsky, G. V.; Kosevich, M. V.; Vovk, M.; Shelkovsky, V. S.; Vashchenko, L. A. *Chem. Commun.* **1995**, *12*, 1281-1282.

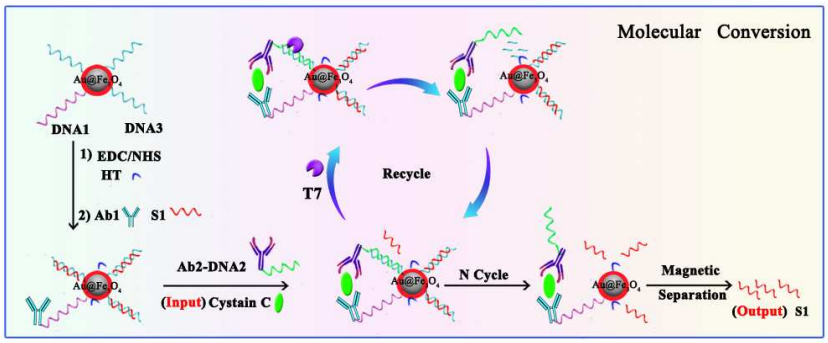
Molecular Conversion
DNA1
DNA3
1) EDC/NHS
HT
2) Ab1
S1
T7
Recycle
Ab2-DNA2
(Input) Cystain C
N Cycle
Magnetic
Separation
(Output) S1

TOC